

## CHARACTERIZATION OF SOLAR NOISE IN IRRADIANCE FROM VIRGO

M. Anklin, C. Fröhlich, W. Finsterle, C. Wehrli  
 Physikalisch-Meteorologisches Observatorium Davos, World Radiation Center  
 CH-7260 Davos Dorf, Switzerland

### ABSTRACT

Fourier analyses of total and spectral solar irradiance show a similar behavior for periods between two minutes and 50 days (0.23 - 8300 mHz) as found in the first result paper with a much shorter time series (Fröhlich et al., 1997). With the extension of the time series, lower frequencies become accessible. With bi- and multivariate spectral analysis the contribution of three spectral channels, 402 nm, 500 nm and 862 nm, to the variance of the total channel are determined. Although the coherence between the different time series is around 75 % for most of the high frequency range, we find a low coherence between 4 and 60  $\mu$ Hz. In this frequency band the instrumental noise dominates the solar noise and the low coherence stems from the individual behaviour of the different instruments, i.e. the absolute radiometers and sun-photometers.

### 1. INTRODUCTION

The continuous measurements from VIRGO (Variability of Solar IRradiance and Gravity Oscillations) onboard the ESA/NASA mission SOHO (Solar and Heliospheric Observatory) allows us to produce power spectra without any modulation sidebands of total and spectral solar irradiance. VIRGO contains two different active-cavity radiometers, PMO6-V and DIARAD, for monitoring the total solar irradiance, and two 3-channel sunphotometer (SPM) for the measurements of the spectral irradiance at 402, 500 and 862 nm with a bandwidth of 5nm. Here, we will mainly use total solar irradiance measurements from PMO6-V and three spectral irradiance channels from SPM. The instrumentation is described in detail in Fröhlich et al. (1995). In the first result paper (Fröhlich et al., 1997) power spectra analyses on time series of 4-6 months were presented. The new analyses performed here on time series which are extended to almost two years duration are in general in agreement with the results from the first result paper.

### 2. POWER SPECTRA ANALYSES

For the frequency analyses we have used level 1 data of total and spectral solar irradiance. Level 1 data

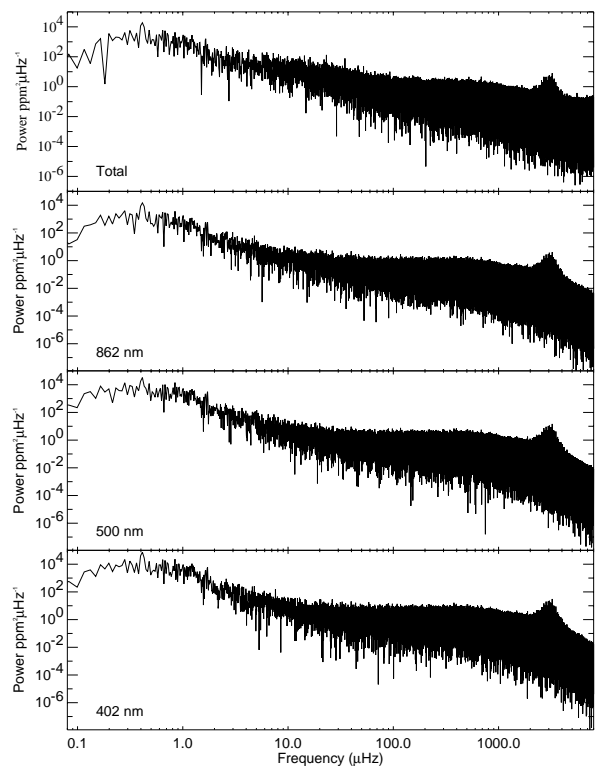


Figure 1. Power spectra of the total and three spectral solar irradiance channels. The power spectra cover the p-mode oscillation (2000-4000  $\mu$ Hz), the granulation (800-3000  $\mu$ Hz), the meso-granulation (80-1000  $\mu$ Hz), and the super-granulation (10-100  $\mu$ Hz).

are corrected for all *a priori* known influences such as distance from the sun, thermal and electrical corrections and the radial velocity to the sun. Data between 1 May, 1996 and 1 April, 1998 (700 days, 1.008 million data points) have been used with one minute resolution and with only few gaps in the time series due to interruption of the experiment. The level 1 data have been detrended with a triangular running average over 60 days (full width) and apodized with a Hanning window to calculate the power spectra shown in Fig. 1. The frequency resolution is

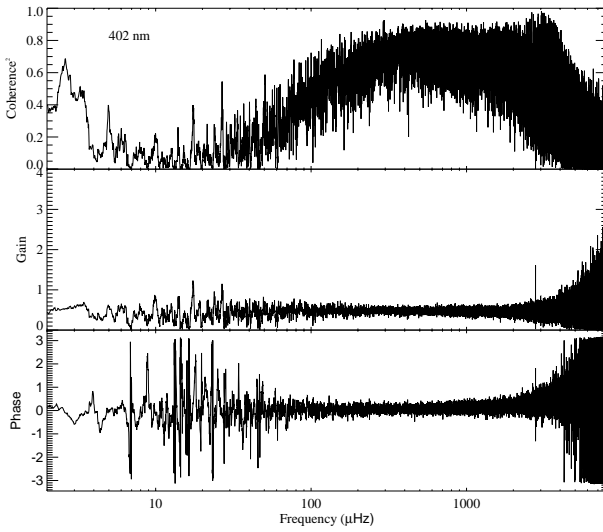


Figure 2. Bivariate analysis between the total and the blue channel. The top panel indicates the coherence squared between the total and the spectral channel. The middle panel shows the gain and the bottom panel shows the phase between the two channels. Note that between 4 and 100  $\mu\text{Hz}$  the coherence squared is very low. This feature will be discussed in more detail in Section 4.

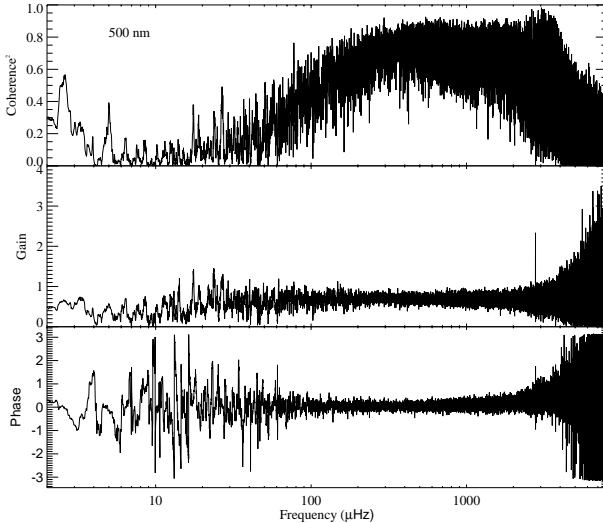


Figure 3. Bivariate analysis between the total and the green channel (see also caption to Fig. 2).

$0.0165 \mu\text{Hz}$  (corresponding to a 700 day period) and the Nyquist frequency is at  $8.33 \text{ mHz}$  (corresponding to a 2 minute period). The power spectra exhibit the prominent p-mode oscillations between 2000 and 4000  $\mu\text{Hz}$ . The granulation covers the interval 800 - 3000  $\mu\text{Hz}$ , the meso-granulation 80 - 1000  $\mu\text{Hz}$ , and the super-granulation 10 - 100 mHz. The g-modes are expected between 10 - 300  $\mu\text{Hz}$ . Since the duty

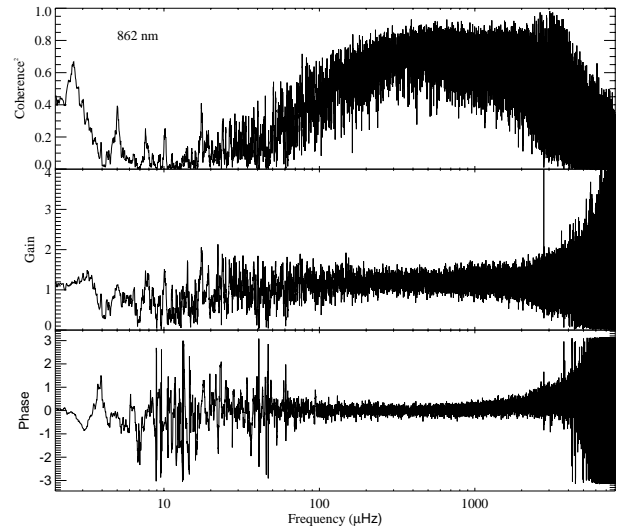


Figure 4. Bivariate analysis between the total and the red channel (see also caption to Fig. 2).

cycle of the SPM is  $>90\%$  and the one of the active cavity radiometer (PMO6-VA) is only 33%, the spectral channels exhibit less noise and no aliasing at high frequency. This illustrates clearly the importance to operate solar radiometers with high duty cycles to get good power analyses in the high frequency range.

### 3. BI- AND MULTIVARIATE ANALYSES

The method of bi- and multivariate spectral analyses is briefly described in Finsterle et al. (1998). Here we calculated bi- and multivariate power spectra between the total and the three spectral channels. The results of the bivariate analyses are shown in Fig. 2-4. For these analyses the power- and cross spectra are calculated by smoothing the Fourier spectra with a running mean of 31 bins ( $0.5 \mu\text{Hz}$ ) and by setting the first and last 16 bins to invalid. Fig. 2-4 show coherence squared, gain, and phase between total and red, green, and blue channels, respectively. The bivariate analyses exhibit high coherence between 2 and 3.5  $\mu\text{Hz}$  and between 100 and 3000  $\mu\text{Hz}$ . At low frequencies this is due to the strong signal of solar activity and at high frequency due to convection and p-mode oscillation. Between 4 and 60  $\mu\text{Hz}$ , however, the coherence is low in all combinations of the four Fourier spectra. Thus, the low coherence squared must come from instrumental behaviour, which is discussed in more detail in Section 4. For frequencies below 4000  $\mu\text{Hz}$ , the average gain in the different bivariate analyses are about 1.20 (red), 0.68 (green) and 0.47 (blue). The phase shows no systematic deviation from zero.

Multivariate analyses allows us to calculate partial coherence between total irradiances, which are modeled simultaneously by the three spectral channels. Using the total channel as dependent and the three spectral channels as independent parameters, we get a similar behaviour for the coherence squared as

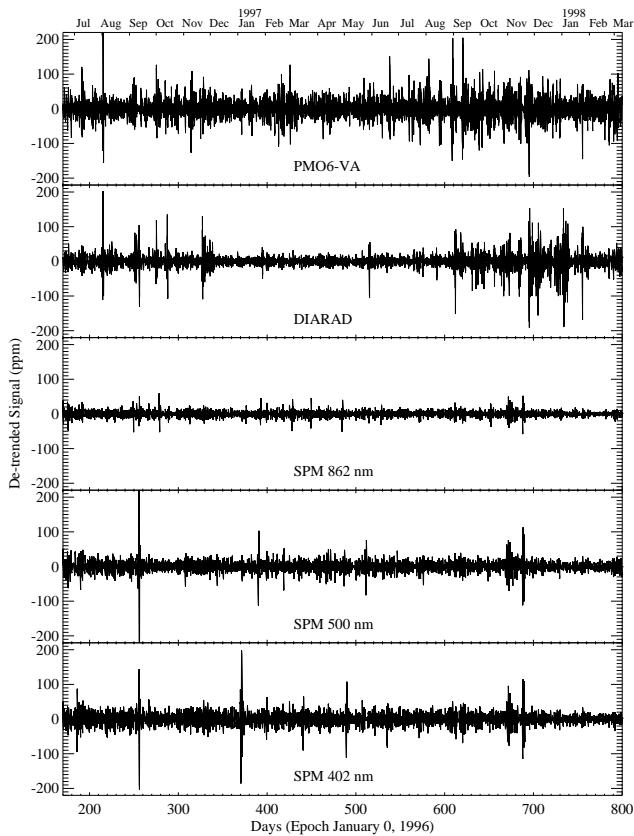


Figure 5. Time series from inverse Fourier transform of the frequency band from 5 - 20  $\mu\text{Hz}$ . This frequency band corresponds to the range with low coherence between the different channels. The inverse transform shows only little similarities between the different time series indicating that the low coherence is indeed due to instrumental effects.

shown in Fig. 2-4. From 0.5 to 3.5  $\mu\text{Hz}$  and 200 to 2000  $\mu\text{Hz}$  75 % of the total spectrum can be explained by the three spectral channels in average, whereas between 4 and 10  $\mu\text{Hz}$  only about 18 % is explained.

#### 4. FILTERED TIME SERIES; LOWPASS BETWEEN 5 AND 20 $\mu\text{Hz}$

To investigate the cause of the low coherence squared in the bivariate and multivariate analyses shown in Fig. 2-4, we calculate inverse Fourier transform for the frequency range between 5 and 20  $\mu\text{Hz}$  (corresponding to periods 14 h to 56 h). The corresponding filtered time series are shown in Fig. 5, where the panels exhibit from top to bottom inverse transform of PMO6-VA, DIARAD, SPM red, green, and blue channel. The time series shown are also corrected for apodization. PMO6-VA exhibits more noise than DIARAD, which is due to different operation modes of the two absolute radiometers; i.e. PMO6-V is 8 h open and 6 min closed, and DIARAD is 1.5 min open and 1.5 min closed. These time series exhibit little

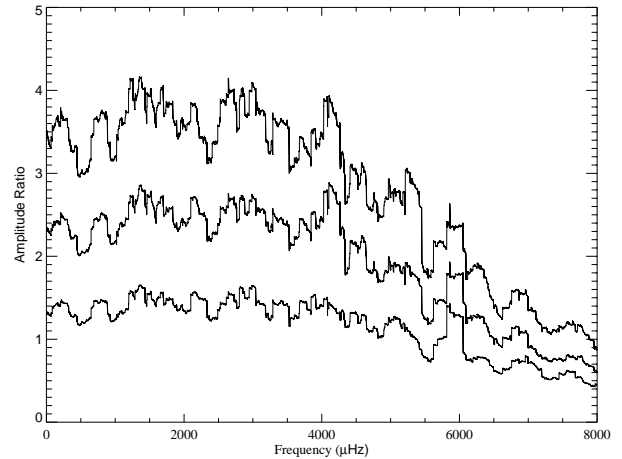


Figure 6. Amplitude ratio of total and the three spectral channels, smoothed with a 14,400 bin running mean (about 240  $\mu\text{Hz}$ ). Up to about 4 mHz the blue channel (upper most curve) exhibits 3-4 times higher amplitudes, the green channel (middle curve) 2-3 times higher amplitudes and the red channel (lower curve) 1-1.5 times higher amplitudes than in the total channel. Above 4 mHz the ratios decrease mainly due to aliasing in the total channel.

similarities between the total and the spectral channels, and there are only few similarities between the SPM channels. This confirms that the noise in the power spectrum (Fig. 1) within this frequency band is indeed due to different instrumental behaviour.

We will use the results of bi- and multivariate analyses to reduce the instrumental noise in the time series and, thus, to get a more accurate determination of the power in solar irradiance data, especially in the frequency range from 4 to 100  $\mu\text{Hz}$ .

#### 5. AMPLITUDE RATIOS OF THE FREQUENCY SPECTRA

The amplitude ratios of the total channel is shown in Fig. 6, smoothed with a 14,400 bin running mean (about 240  $\mu\text{Hz}$ ). Similar to the first result paper (Fröhlich et al., 1997) we find about 3 to 4 times higher amplitudes in the blue channel, about 2 to 3 times higher amplitudes in the green channel, and about 1 to 1.5 times higher amplitudes in the red channel than in the total channel. In the first result paper Fröhlich et al. (1997) found rather constant ratios for the frequency range of granulation and meso-granulation, whereas a broad hump was observed between about 3 to 20  $\mu\text{Hz}$ . While extending the time series to nearly two years, we find similar amplitude ratios although the broad hump can not be confirmed. The amplitude ratios between 0 and 4000  $\mu\text{Hz}$  show no large variations. As shown above most of the power between 3 to 20  $\mu\text{Hz}$  stems from instrumental noise and, therefore, the broad hump in the first result paper is due to different instrumental behaviour, which is now averaged out in the longer time series. Towards higher frequencies, i.e. above about 4000  $\mu\text{Hz}$ , the ratios decrease, which is mainly due to aliasing of the Fourier spectrum of the total irradiance due to the low duty cycle.

## 6. CONCLUSIONS

Throughout most of the high frequency spectrum 75% of the variations of the total solar irradiance can be explained by the three spectral channels (862 nm, 500 nm, 402 nm). However, between 4 and 20  $\mu\text{Hz}$  only 17 % of the total spectrum can be modeled by the spectral channels. The low coherence in this frequency band is due to differences of the behaviour of the instruments; irregular and among the instruments uncorrelated spikes in the data produce this noise spectrum. As shown in Fig. 1, the meso-granulation does not add to the solar noise. Between 10 and 100  $\mu\text{Hz}$  the increase in power is partly due to instrumental noise and only about 10 to 30 % of the increase stems from super-granulation. At low frequencies below 4  $\mu\text{Hz}$  the coherence is again high indicating that the variance due to solar activity is much larger than the instrumental effects.

## ACKNOWLEDGEMENTS

The authors gratefully acknowledge the past and on-going effort of the VIRGO team to produce and interpret the data. SOHO is a mission of international cooperation between ESA and NASA. This work at the PMOD/WRC is funded by the Swiss National Foundation.

## REFERENCES

- Finsterle, W. and Fröhlich, C.: 1998, in S. Korzenik and A. Wilson (eds.), *Structure and Dynamics of the Interior of the Sun and Sun-Like Stars*, p. this volume, ESA SP-418, ESA Publications Division, Noordwijk, The Netherlands
- Fröhlich, C., Andersen, B., Appourchaux, T., Berthomieu, G., Crommelynck, D. A., Domingo, V., Fichot, A., Finsterle, W., Gómez, M. F., Gough, D. O., Jiménez, A., Leisen, T., Lombaerts, M., Pap, J. M., Provost, J., Roca Cortés, T., Romero, J., Roth, H., Sekii, T., Telljohann, U., Toutain, T., and Wehrli, C.: 1997, *Sol.Phys.* **170**, 1
- Fröhlich, C., Romero, J., Roth, H., Wehrli, C., Andersen, B. N., Appourchaux, T., Domingo, V., Telljohann, U., Berthomieu, B., Delache, P., Provost, J., Toutain, T., Crommelynck, D., Chevalier, A. and Fichot, A., Däppen, W., Gough, D. O., Hoeksema, T., Jiménez, Gómez, M., Herberos, J., Roca-Cortés, T., Jones, A. R., and Pap, J. and Willson, R. C.: 1995, *Sol.Phys.* **162**, 101